COMPDYN 2011
III ECCOMAS Thematic Conference on
Computational Methods in Structural Dynamics and Earthquake Engineering
M. Papadrakakis, M. Fragiadakis, V. Plevris (eds.)
Corfu, Greece, 25–28 May 2011

OPTIMAL WHOLE-LIFE-CYCLE SEISMIC DESIGN OF CONCRETE FRAMES

Bora Gencturk[1] **and Amr S. Elnashai**[2]

[1] University of Illinois at Urbana-Champaign
Department of Civil and Environmental Engineering, 1240 Newmark Lab, 205 N Mathews Ave, Urbana, IL, 61801
e-mail: bgenctu2@illinois.edu

[2] University of Illinois at Urbana-Champaign
Department of Civil and Environmental Engineering, 1114 Newmark Lab, 205 N Mathews Ave, Urbana, IL, 61801
email: aelnash@illinois.edu

Keywords: Reinforced concrete, ECC, dynamic analysis, structural optimization, Pareto-front, Life-cycle cost analysis.

Abstract. *In this study multi-objective optimization of structural frames is investigated. Two different materials, reinforced concrete and reinforced engineered cementitious composites (ECC), with different response characteristics are used to model the frames. ECC is characterized by high tensile strength and ductility, high energy absorption and reduced crack widths when compared to conventional concrete. However, the material is more expensive than conventional concrete. Therefore, in order to quantify the potential benefits that could be obtained by replacing concrete with ECC, the structural performance is evaluated for the whole-life-cycle of the structure. The results of the optimization problem are presented in Pareto-optimal form which is preferred by decision makers due to the provided flexibility in selecting the solution alternatives. The option of replacing the conventional material, concrete, with a high performance alternative, ECC, is investigated in an optimization framework with the ultimate goal of higher safety, increased sustainability and improved performance.*

1 INTRODUCTION

Optimal and sustainable design of structures has become an important issue in the recent years. Through the use of optimization techniques, it is possible to reduce the material usage, hence environmental impacts, and concurrently prevent failures by better understanding the structural behavior at different limit states. This paper investigates the use of a high-performance material, engineered cementitious composites (ECC), to reduce the life-cycle cost (LCC) of concrete frames and improve the structural performance at different limit states.

ECC is a fiber-reinforced high-performance material introduced as a replacement for concrete by Li and co-workers [1-4]. ECC differs from other types of high-performance cementitious materials in that the microstructures are optimized using micromechanical models to achieve ultra-high ductility, with crack widths limited to below 100μm and ultimate tensile strain capacity as high as 5 percent [5]. The improved performance of ECC comes with an increased cost and reduced greenness. The ECC mixtures are less environmental friendly and cost 1.5-3.3 times more than concrete. However, the seismic structural performance of ECC evaluated in terms of stiffness, strength, ductility and energy absorption capacity is significantly higher [6]. Therefore, the material has to be utilized in the most efficient way to reduce the LCC, increase sustainability through less material usage and extended lifetime, and improve safety through higher performance. This is best investigated by defining an optimization problem that includes structural response in addition to initial and whole-life-cycle costs as the primary objectives.

In the following, a multi-objective optimization problem is formulated taking into account the structural performance, and the initial and whole life-cycle costs. In order to utilize the ECC material in the most efficient way, the critical (potential plastic hinge) locations of the structural frames, i.e. beam-column connections and bases of the columns are deployed with ECC and for the rest of the structure conventional concrete is used. Here, these are referred as multi-material (MM) frames. To assess the performance of this intervention strategy, the results are compared to those of the frames made of concrete only and ECC only.

The ground motions that are used for inelastic dynamic time history analysis of the structural frames are derived by probabilistic seismic hazard analysis (PSHA) at a selected site. This computationally intensive inelastic dynamic time history analysis is employed so as to accurately obtain the earthquake demand and to distinguish the response of reinforced concrete (RC) and ECC frames from that of MM frames. The structural capacity is evaluated by pushover analysis and local response measures, strains in longitudinal reinforcement and matrix (concrete or ECC), are used to define the limit states. The optimal solutions in the search space are found by a Taboo search algorithm which is shown to be very efficient in solving combinatorial problems. The results are presented in Pareto-optimal form to provide flexibility in selecting the alternative solutions and to compare the performance of different frames in the objective function space.

2 SEISMIC HAZARD AND EARTHQUAKE GROUND MOTIONS

2.1 Definition of the seismic hazard

In this study uniform hazard spectra (UHS) obtained from PSHA are used to characterize the seismic hazard for a selected site. The UHS used here are based on the developments by U.S. Geological Survey (USGS) on 2008 national seismic hazard mapping [7].

A site at the intersection of 2nd and Market Streets in San Francisco, CA (with coordinates 37° 47′ 21.58′′ N, 122° 24′ 04.77′′ W) is selected and the seismic hazard is consistently de-

rived. The sources of seismicity contributing to the hazard at the selected site are shown in Figure 1(a). The governing faults for the selected site are the San Andreas, the San Gregorio and the Hayward faults. The source-to-site distance varies between 11 km to 25 km depending on the fault. The soil conditions might significantly alter the characteristics of the ground motions at a site, therefore, the soil conditions are also taken into account in the development of UHS. The soil at the selected site is determined as D on the NEHRP [8] scale with a shear wave velocity in the range from 180 m/sec to 360 m/sec.

Site specific hazard curve for peak ground acceleration (PGA), and UHS for three different return periods (i.e. 75, 475, and 2475 years) are calculated as shown in Figure 3(a) and (b), respectively. These return periods correspond to three structural limit states: immediate occupancy (IO), life safety (LS) and collapse prevention (CP), respectively.

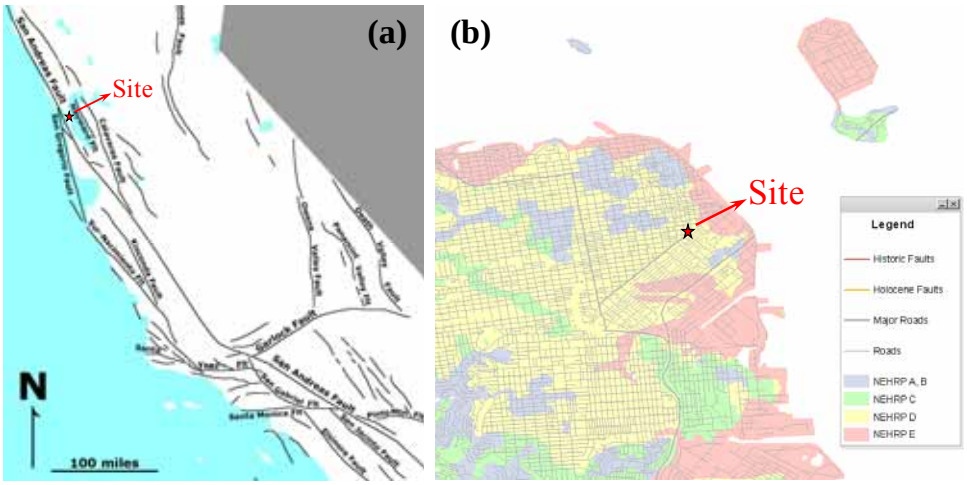

Figure 1: (a) Sources of seismicity [9], and (b) soil profile at the selected site [10].

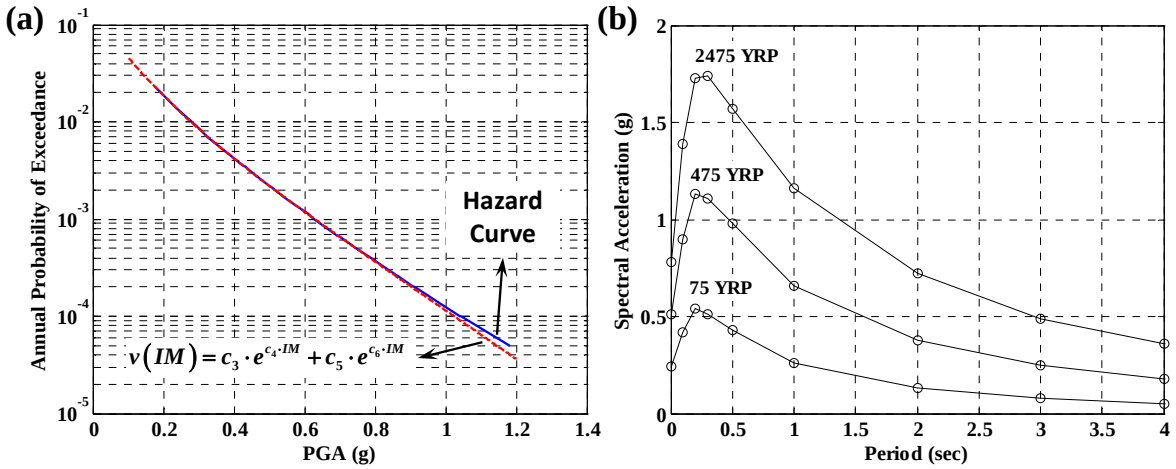

Figure 2: (a) PGA hazard curve, and (b) UHS at different return periods (YRP stands for years return period).

2.2 Selection and spectrum matching of the earthquake ground motions

The disaggregation is performed in order to determine the relative contribution of seismic sources to hazard at a particular location. As a result of the disaggregation calculations the significant parameters, i.e. magnitude, distance, and PGA that characterize the seismic hazard are determined. These values together with the soil conditions and UHS control the selection of earthquake time histories that are used for seismic design and assessment purposes.

The PEER NGA database [11] is utilized to select seven earthquake recordings are for each of the three return periods. The following criteria are used for selecting the records: (1) earthquakes having similar mechanisms to those which are pertinent to the faults affecting the site, (2) magnitudes within ±1 with the governing magnitude for the considered return period, (3) shear wave velocity of the recording station within the range from 180 m/sec to 360 m/sec, and (4) the acceleration spectrum of the earthquake time history matching as closely as possible the UHS associated with the considered return period.

Spectrum matching is utilized to make the selected ground motions compatible with the UHS at different return periods. For this purpose the RSPMatch software [12] is utilized. The relevant period range for the structural frames considered in this study is from 0-1 sec (see Section 3.1). Therefore, in order not to introduce unrealistic low frequency oscillations in the spectrum compatible ground motions, when target spectra are defined the original spectra of the records are retained for periods longer than 1 sec, and UHS are used for periods shorter than 1 sec. The response spectra, and the acceleration time history before and after spectrum matching of an example record for 475 years return period are shown in Figure 3(a) and (b), respectively.

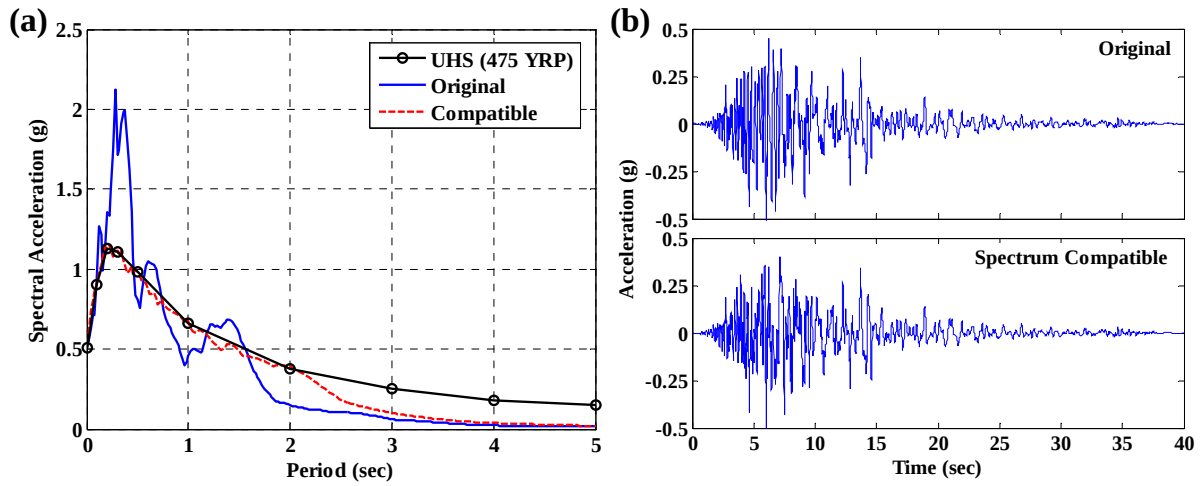

Figure 3: (a) UHS, and response spectrum, and (b) acceleration time history of the selected record, before and after spectrum matching for the 475 years return period.

3 DESCRIPTION OF THE MULTI-OBJECTIVE OPTIMIZATION PROBLEM

3.1 Structural frames

The frame considered for structural optimization is illustrated in Figure 4. The critical locations, i.e. beam-column connections and the column bases are made of ECC, while the rest of the frame is concrete. One tenth of the members' length on each side is assumed to be the critical regions. As mentioned earlier RC only and ECC only frames are also considered for comparison purposes. Seven design variables are defined for the optimization problem as given in Table 1, alongside the minimum and maximum values and increments. The combination of these design variables results in 30,000 cases which constitute the search space for each frame type.

The initial cost of the frames considers only the material costs. The unit prices for concrete and steel are assumed to \$0.13/liters and \$0.66/kg, respectively. It is assumed that the struc-

tural members are properly designed to prevent shear failure and the amount shear reinforcement is calculated following a capacity design approach. First, the moment capacity of the sections are calculated and increased by 20 percent to account for overstrength. Then, the shear force that produces the moment capacity is evaluated and the required shear reinforcement is calculated according to ACI-318 [13]. The cost of shear reinforcement is also included in the initial cost of the frames. It is demonstrated through experimental studies that the shear reinforcement can be eliminated for flexural ECC members [6]. Therefore, no shear reinforcement is added to sections where ECC is used. Labor costs are not considered in this study.

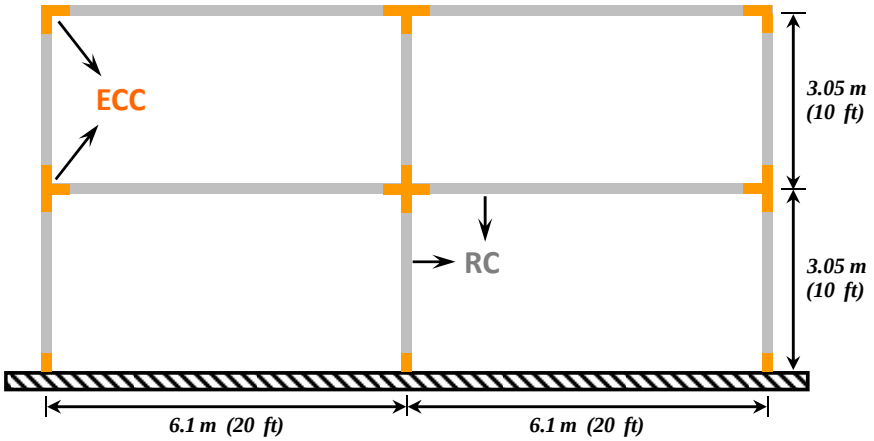

Figure 4: The considered structural frame for optimization.

	Minimum	Maximum	Increment
Column Reinforcement Ratio	1.0%	2.5%	0.50%
Beam Reinforcement Ratio	0.5%	2.0%	0.50%
Width of Exterior Columns (mm)	660.4	863.9	50.8
Width of Interior Columns (mm)	711.2	914.4	50.8
Width of Columns (mm)	457.2	660.4	50.8
Depth of Beams (mm)	508	711.2	50.8
Depth of Beams (mm)	406.4	508	50.8

Table 1: Design variables and ranges for the considered structural frames.

3.2 Evaluation of structural capacity and earthquake demand

Structural capacity is evaluated by pushover analysis. The frames described in Section 3.1 are modeled using fiber-based finite element analysis software ZEUS NL [14] which includes a validated constitutive model for ECC [6]. The three structural limit states, IO, LS and CP that correspond to the three return periods, 75, 475 and 2475 years are determined from the pushover analysis using local response measures, i.e. strains in concrete and longitudinal reinforcement. Based on previous research on testing of steel reinforcement and concrete [15], the occurrence of IO and LS limit states are defined as the reaching or exceeding 0.5 and 5 percent strain, respectively, in the reinforcing steel of any of the columns or beams. The occurrence CP limit state is defined as reaching or exceeding 10 percent strain in reinforcing steel or 1 percent compressive strain in core concrete in any of the columns or beams.

In order to establish the mean values for the limit states to be used in the LCC model, 50 cases are selected randomly from the 30,000 combinations. Pushover analyses of the RC, MM and ECC frames are conducted and the limit states are found in terms of interstory drift.

The selected cases are also utilized to quantify the dispersion in earthquake demand due to variability in the ground motion which is a critical parameter for LCC calculation. Each of the previously mentioned 50 cases is subjected seven ground motions (using inelastic dynamic time history analysis) for each return period. A lognormal distribution is fitted to the earthquake demand at each return period and for each frame type to obtain the dispersion values (β_D in Section 3.3). It is seen that the dispersion in earthquake demand increases for increasing hazard level (return period). 0.25, 0.35 and 0.45 are used as to describe the dispersion in earthquake demand at return periods of 75, 475 and 2475 years, respectively.

3.3 Derivation of the life-cycle cost model

The LCC of a structure (due to post earthquake repair) is a critical parameter for structural engineers and decision makers such as owners. Therefore, it is important to include the LCC as one of the objectives in optimal seismic design of structures. The expected LCC of a structure is calculated as [16]

$$E\left[C_{LC}(t)\right] = C_0 + \frac{\left(1-e^{-\lambda t}\right)}{\lambda}\sum_{i=1}^{N} C_i P_i \tag{1}$$

where C_0 is the initial construction cost, t is the service life of the structure (here taken as 75 years), λ is the constant discount rate per year that converts costs due to hazard that occurs in the future into present value (taken as 1 percent), N is the total number of limit-states considered (here equal to 3), P_i is the probability that the structure will be in the ith damage state given the earthquake occurrence, and C_i is the corresponding cost as a fraction of the initial cost of the structure. P_i is given by

$$P_i = P\left(\Delta_D > \Delta_{C,i}\right) - P\left(\Delta_D > \Delta_{C,i+1}\right) \tag{2}$$

where Δ_D is the earthquake demand and $\Delta_{C,i}$ is the structural capacity, in terms of drift ratio, defining the ith damage state as described in Section 3.2. The probability of demand being greater than capacity is evaluated as

$$P\left(\Delta_D > \Delta_{C,i}\right) = \int_0^\infty P\left(\Delta_D > \Delta_{C,i} \mid IM = im\right)\left|\frac{dv(IM)}{dIM}\right| dIM \tag{3}$$

where the first term inside the integral is the conditional probability of demand being greater than the capacity given the ground motion intensity, *IM*. This term is also known as the fragility function. The second term is the slope of the mean annual rate of exceedance of the ground motion intensity. The hazard curve defined as *v(IM)* in Eqn. (3), where *IM* is PGA for this study, is shown in Figure 2(a). The conditional probability of demand being greater than the capacity is

$$P\left(\Delta_D > \Delta_{C,i} \mid IM = im\right) = \int_0^\infty P\left(\Delta_D > \delta \mid IM = im\right) f_C(\delta)\, d\delta \tag{4}$$

where δ is the variable of integration and f_C is the probability density function for structural capacity. This formulation assumes that the demand and the capacity are independent of each other. Structural capacity is assumed to be lognormally distributed with $\Delta_{C,i}$ and β_C that are, respectively, the mean and the standard deviation of the corresponding normal distribution. $\Delta_{C,i}$ is evaluated as described in Section 3.2 for RC, MM and ECC frames. The structural de-

mand is also assumed to follow a lognormal distribution and the probability of demand exceeding a certain value, δ, is given by

$$P\left(\Delta_D > \delta \mid IM = im\right) = 1 - \Phi\left[\frac{\ln\left(\delta\right) - \lambda_{D|IM=im}}{\beta_D}\right] \tag{5}$$

where $\Phi[\cdot]$ is the standard normal cumulative distribution, λ_D is the natural logarithm of the mean of the earthquake demand as a function of the ground motion intensity, and β_D is the standard deviation of the corresponding normal distribution of the earthquake demand. Although, β_C and β_D are dependent on ground motion intensity, in most studies they are taken as constants due to lack of information. The uncertainty in capacity (here represented with β_C) due to sources such as modelling error, lack of knowledge and variation in material properties was investigated in several studies [17]. In this study it is assumed to be equal to 0.35 taking previous research as a reference [17]. The dispersion in earthquake demand (here represented with β_D) due to variability in ground motions is evaluated here as described in Section 3.2. The mean of earthquake demand, μ_D, as a continuous function of the ground motion intensity is described using

$$\mu_D\left(IM\right) = c_1 \cdot IM^2 \tag{6}$$

where the constant c_1 is determined by curve fitting to the three data points that match the PGA of the ground motions records at return periods 75, 475 and 2475 years with the earthquake demand evaluated using inelastic dynamic analysis.

The hazard curve shown in Figure 2(a) is also described in the mathematical form

$$v\left(IM\right) = c_3 \cdot e^{c_4 \cdot IM} + c_5 \cdot e^{c_6 \cdot IM} \tag{7}$$

where c_3 through c_6 are constant to be determined from curve fitting. The results of the curve fitting using the functional form described by Eqn. (7) to the PGA hazard curve at the selected site is shown in Figure 2(a).

With the above described formulation each term in Eqn. (3) is represented as an analytical function of the ground motion intensity, *IM*. Thus, using numerical integration the desired probabilities of Eqn. (2) can easily be calculated. The LCC is evaluated through Eqn. (1).

4 TABOO SEARCH ALGORITHM

As described earlier the optimization problem is reduced to a combinatorial one due to discrete nature of the design variables. Taboo search (TS) algorithm which is known to be very efficient in solving combinatorial problems is used here.

To describe the modified TS algorithm used here, first, it is required to make the following definitions. The taboo list includes points in the design space for which the objective functions are evaluated for. Since inelastic dynamic time history analysis is computationally costly, this list is used to avoid multiple runs with the same combination of design variables. That is, a point in the taboo list is not evaluated again. The Pareto list includes the points that are not dominated by other points within the set for which the evaluation of objective functions is performed (i.e. the taboo list). The seed list includes the points around which optimal solutions are looked for. The latter are called as the neighboring points and they are basically the adjacent elements of the multidimensional array, that defines the decision (or design) variables, around the given seed point. The modified TS algorithm works as follows:

a. Start with the minimum cost combination evaluate the objective function and add this point into taboo, seed and Pareto lists. Use this point as the initial seed point.
b. Find the neighboring points around the current seed. Here the number of neighboring points is chosen equal to the number of design variables and selected randomly amongst all the adjacent elements of the multidimensional array that defines the design variables.
c. Evaluate the objective function for all the neighboring points and add these into taboo list.
d. Find the Pareto-front using the set of points for which the objective function is evaluated and update the Pareto list as the current Pareto-front.
e. Amongst the neighboring points for the current iteration choose the one that is on the Pareto-front and minimizes the cost function as the next seed point and add this point into the seed list. If there is no point which satisfies these conditions choose randomly one of the points from the Pareto list amongst the ones that are not already in the seed list.
f. Check if the predetermined maximum number of objective function evaluations is exceeded; if yes stop, if not go to Step b.

5 RESULTS AND DISCUSSION

As an example of how the TS algorithm conducts the search within the search space, in Figure 5(a), the results for initial cost vs. maximum interstory drift for the MM frame at 2475 years return period is shown. It is seen that the TS algorithm is very efficient in narrowing down the search space to the points that are close to the Pareto-front, which is shown with solid line with circle marks. In Figure 5(b), the Pareto-fronts at the three hazard levels are compared for the MM frame. These results are very useful for decision makers. It allows the decision maker, whether it is the owner or the engineer, to choose among the set of optimal solutions depending on the requirements of the project. As an example, if the requirement of the project is that the maximum interstory drift under the 2475 years return period earthquake is less than four percent, one can easily find the least cost solution. Later on, if the requirement of the project changes and it becomes necessary to limit the maximum interstory drift to three percent, no additional analysis will be required to find the optimal solution.

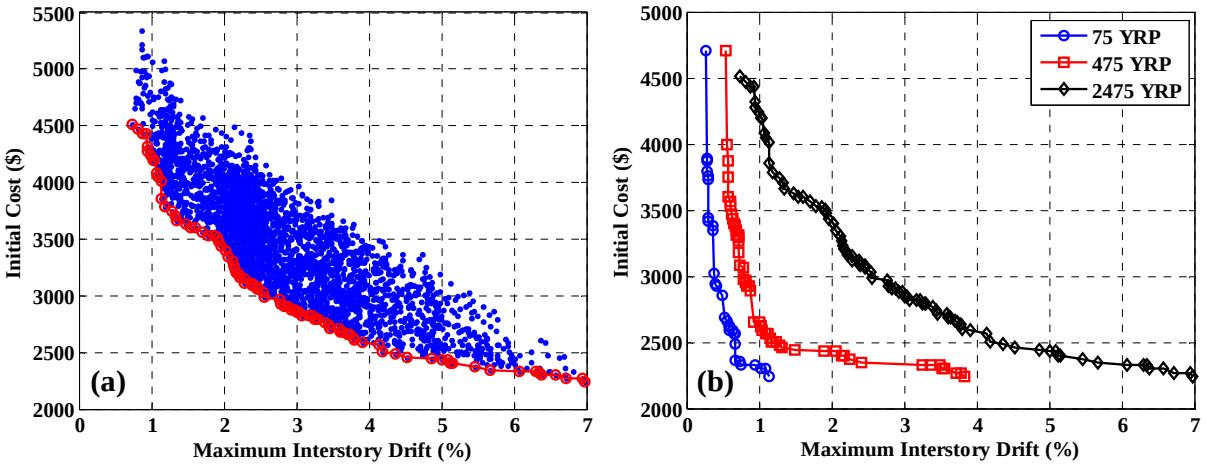

Figure 5: (a) Initial cost vs. maximum interstory drift for the MM frame at 2475 years return period, (b) Pareto-fronts for different return periods – MM frame.

As shown in Figure 6(a), in terms of total cost, the MM frame performs slightly better than RC frame due to reduced repair cost resulting from the increase in structural capacity as described in Section 3.2. However, as mentioned in Section 3.1, for simplicity in calculation of the initial cost, the workmanship costs are not included, and the initial cost is solely based on the material cost. In other words, the reduction in workmanship costs due to reduction in reinforcement detailing and prevention of congestion problems that result from the elimination of shear reinforcement is not taken into account. Furthermore ECC material is proven to be more durable than conventional concrete due to reduced crack widths with a distributed cracking pattern which increases the lifetime of the buildings [18, 19]. MM frame performs better when this additional information is taken into account. It is seen in Figure 6(a) that with the ECC frame the maximum interstory drift could be lowered to levels which cannot be achieved with the RC or MM frames. The Pareto-fronts for repair vs. initial cost for the three frames are compared in Figure 6(b). It is seen that the repair cost of the ECC frame is significantly less compared to RC frame for similar initial costs. The repair cost of the ECC frame is higher as it is based on the higher initial material cost.

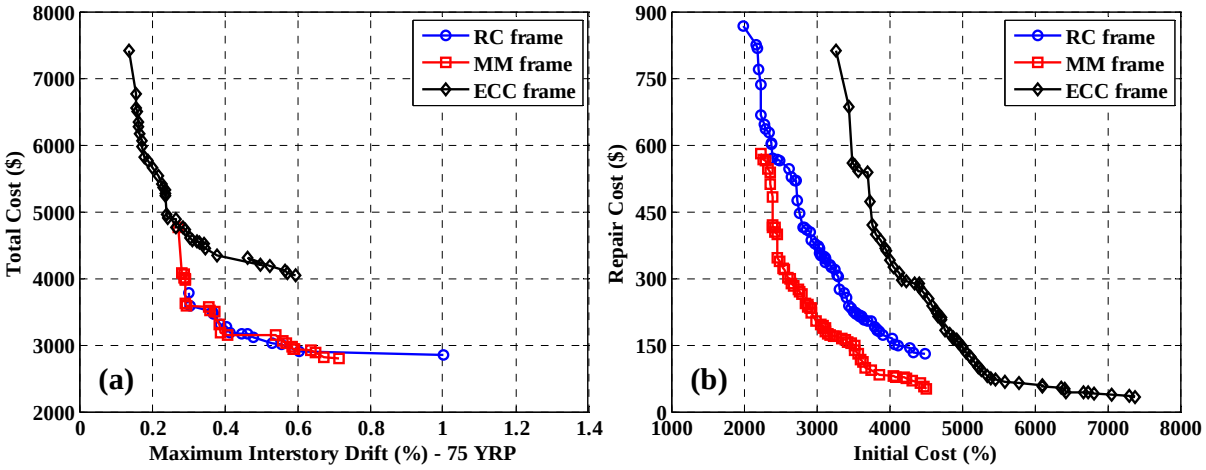

Figure 6: Pareto fronts for the three frames (a) total (life-cycle) cost vs. maximum interstory drift at 75 years return period, (b) repair cost vs. initial cost.

The seismic LCC analysis poses significant challenges to researchers. There are various parameters that have direct effect on the LCC results. Most importantly, for the formulation provided in this paper, the constants C_i in Eqn. (1) which define the cost of repair for the i^{th} damage state as a fraction of the initial cost have strong influence on the LCC. It is not straightforward to determine damage states for structures and the associated cost for repair. Furthermore, based on the adopted definitions, the limit state threshold values may vary significantly which affects the failure probabilities. Eqn. (4) assumes that the structural capacity is independent of earthquake demand which is another simplification that is usually adopted. Finally, the evaluation of workmanship cost is difficult as it is dependent on various parameters, above all the cost of labor at the location of construction. These are the most important assumptions of this study that warrant further investigation in the future studies.

6 CONCLUSIONS

The use of engineered cementitious composite (ECC) materials for improving the seismic design of buildings in terms of safety, economy and sustainability, is investigated through a multi-objective optimization problem. The objectives are selected as the structural performance, initial and the life-cycle cost (LCC). Three types of structural frames are considered:

made from reinforced concrete (RC) and reinforced ECC only, and a multi-material (MM) frame where the ECC is only used at the beam-column connections and at the bases of the columns. It is observed that, although the earthquake demand is significantly reduced in the case of ECC frame, the gain is not justified due to increased initial cost. On the other hand, the structural capacity of the MM frame is significantly higher which results in reduced repair hence LCC. If the additional benefits such as the reduction in workmanships costs and increased in life-time with enhanced ECC material durability are taken into account, the MM frame come forward as the most optimal solution to achieve the multiple objectives of the problem.

REFERENCES

[1] Li, V.C., *Postcrack Scaling Relations for Fiber Reinforced Cementitious Composites.* Journal of Materials in Civil Engineering, 1992. **4**(1): p. 41-57.

[2] Li, V.C. *Performance Driven Design of Fiber Reinforced Cementitious Composites*. in *4th International Symposium on Fiber Reinforced Concrete*. 1992: Chapman and Hall.

[3] Li, V.C. and C.K.Y. Leung, *Steady-State and Multiple Cracking of Short Random Fiber Composites.* Journal of Engineering Mechanics, 1992. **118**(11): p. 2246-2264.

[4] Li, V.C. and H.C. Wu, *Conditions for Pseudo Strain-Hardening in Fiber Reinforced Brittle Matrix Composites.* Journal of Applied Mechanics Review, 1992. **45**(8): p. 390-398.

[5] Li, V.C., S. Wang, and C. Wu, *Tensile Strain-Hardening Behavior of Polyvinyl Alcohol Engineered Cementitious Composite (PVA-ECC).* ACI Materials Journal, 2001. **98**(6): p. 483-492.

[6] Gencturk, B., *Multi-Objective Optimal Seismic Design of Building Using Advanced Engineering Materials*, in *Department of Civil and Environmental Engineering*. 2011, University of Illinois at Urbana-Champaign: Urbana, IL.

[7] USGS. *Documentation for the 2008 Update of the United States National Seismic Hazard Maps,* Open-File Report 2008-1128, 2008, United States Geological Survey, Reston, Virginia, USA.

[8] FEMA. *NEHRP Recommended Provisions for Seismic Regulations for New Buildings and Other Structures, FEMA 450, Part 1: Provisions*, 2003, Federal Emergency Management Agency, Washington, District of Columbia.

[9] U.S. Geological Survey. *Major Faults of California*. 2009, Accessed on May 13, 2009. Available from: http://education.usgs.gov/california/maps/faults_names3.htm.

[10] U.S. Geological Survey. *Soil Type and Shaking Hazard in the San Francisco Bay Area*. 2009, Accessed on February 1, 2011. Available from: http://earthquake.usgs.gov/regional/nca/soiltype/.

[11] PEER. *Pacific Earthquake Engineering Research (PEER) Center: NGA Database*. 2005, Accessed on January 1, 2009. Available from: http://peer.berkeley.edu/nga/.

[12] Abrahamson, N., *Non-Stationary Spectral Matching.* Seismological Research Letters, 1992. **63**(1): p. 30.

[13] ACI, *Building Code Requirements for Structural Concrete (ACI 318-08) and Commentary*. 2008, American Concrete Institute, Farmington Hills, MI, USA.

[14] Elnashai, A.S., V.K. Papanikolaou, and D. Lee. *ZEUS NL - A System for Inelastic Analysis of Structures,* User's Manual, 2010, Mid-America Earthquake (MAE) Center, Department of Civil and Environmental Engineeering, University of Illinois at Urbana-Champaign, Urbana, IL.

[15] Goodfellow, R.G.C., *Ductility of Reinforced Concrete Flexural Members Constructed from High Performance Steel and Concrete*, in *Civil Engineering Department*. 1999, Imperial College of Science, Technology and Medicine: London.
[16] Wen, Y.K. and Y.J. Kang, *Minimum Building Life-Cycle Cost Design Criteria. I: Methodology.* Journal of Structural Engineering, 2001. **127**(3): p. 330-337.
[17] Wen, Y.K., B.R. Ellingwood, and J.M. Bracci. *Vulnerability Function Framework for Consequence-Based Engineering,* Project DS-4 Report, 2004, Mid-America Earthquake (MAE) Center, Urbana, IL.
[18] Lepech, M.D. and V.C. Li. *Durability and Long Term Performance of Engineered Cementitious Composites*. in *International RILEM Workshop on High Performance Fiber Reinforced Cementitious Composites in Structural Applications*. 2006: RILEM Publications SARL.
[19] Li, V.C., T. Horikoshi, A. Ogawa, S. Torigoe, and T. Saito, *Micromechanics-Based Durability Study of Polyvinyl Alcohol-Engineered Cementitious Composite.* ACI Materials Journal, 2004. **101**: p. 242-248.